Photoinduced modification of surface states in nanoporous InP

J. Lloyd-Hughes,[1,a)] S. Müller,[1,2] G. Scalari,[2] H. Bishop,[3] A. Crossley,[3] M. Enachi,[4] L. Sirbu,[4] and I. M. Tiginyanu[4]
[1]*Department of Physics, Clarendon Laboratory, University of Oxford, Parks Road, Oxford OX1 3PU, United Kingdom*
[2]*ETH Zürich, Institute for Quantum Electronics, Wolfgang-Pauli-Strasse 16, 8093 Zürich, Switzerland*
[3]*Materials Department, Oxford University, Parks Road, Oxford OX1 3PH, United Kingdom*
[4]*National Center for Materials Study and Testing, Technical University of Moldova and Laboratory of Nanotechnology, Institute of Electronic Engineering and Nanotechnologies, Academy of Sciences of Moldova, Chisinau 2004, Republic of Moldova*

(Received 11 November 2011; accepted 7 March 2012; published online 29 March 2012)

Porous honeycombs of n-type InP were investigated by terahertz time-domain and x-ray photoemission spectroscopies. After photoexcitation the dark conductivity was found to increase quasi-irreversibly, recovering only after several hours in air. The calculated electron density for different surface pinning energies suggests that photoexcitation may reduce the density of surface states. © *2012 American Institute of Physics*. [http://dx.doi.org/10.1063/1.3697410]

A precise control of the surface properties of semiconductor nanomaterials is vital for their functionality and use in many opto-electronic applications. Porous semiconductors[1] have been investigated as birefringent[2] and non-linear optical media[3,4] and as emitters of terahertz radiation.[4,5] Giant surface areas and high aspect ratios makes them attractive as functionalized surfaces in biochemical sensors.[6,7] Terahertz time-domain spectroscopy allows the non-contact investigation of electron transport in semiconductor nanomaterials[8] and has been used to determine the equilibrium and photoconductivity of porous InP.[9,10] The technique allows the photoconductivity to be determined on picosecond timescales, provided that the material's properties are not permanently altered by photoexcitation.

In this article, we report that the photoexcitation of nanoporous InP honeycombs quasi-permanently increases the conductivity of the material, with the conductivity remaining high over 1 h after the photoexcitation beam is blocked. Terahertz time-domain spectroscopy was used to measure the transmission of InP porous membranes with varying donor density and orientation. Calculations and x-ray photoemission spectroscopy (XPS) were utilized to examine the charge density and composition of surface states.

Porous InP honeycombs were produced by the electrochemical etching[1,11] of ⟨100⟩ and ⟨111⟩ oriented n-type InP (with a donor density of either $N_1 = 1 \times 10^{17}$ cm^{-3} or $N_2 = 9 \times 10^{18}$ cm^{-3}), producing curropores perpendicular to the samples' surfaces. In Fig. 1(a), typical scanning electron micrographs are shown for curropores running normal to the surface of the low doping (left) and high doping (right) substrates. While the areal fill fraction f is comparable for the two samples, the width of the InP walls is 125 ± 5 nm for the low doping case and 48 ± 7 nm for the high doping case. Cross-sectional electron microscopy images verified that the pores had uniform diameter and extended throughout the sample's thickness ($d = 32\,\mu$m for high doping and $d = 50\,\mu$m low doping).

In order to investigate dc current flow over macroscopic in-plane distances, current-voltage characteristics were obtained from electrically contacted devices. Initially the current at low voltages is a few nA, as the solid line in Fig. 1(b) illustrates for ⟨111⟩-oriented, $N_d = 9 \times 10^{18}$ cm^{-3} pores in a sweep from 0 V to 10 V taking 1 s. This is many orders of magnitude below the current for a bulk reference sample with the same doping (data not shown), which was 75 mA at 0.1 V. Macroscopic transport is hindered in porous InP by the proximity of the surface, which depletes the material of electrons (see below). At higher voltages, the current flow in the porous samples is unstable, and a step increase is witnessed at 5 V. The second current-voltage characteristic (dashed line) exhibits a higher current at low voltages. Repeated sweeps (not shown) have shapes similar to the second sweep, while if the samples are left in air for a couple of minutes without bias then the initial characteristic is obtained upon repeating the experiment. This behaviour suggests that the injection of energetic electrons alters the conductivity of

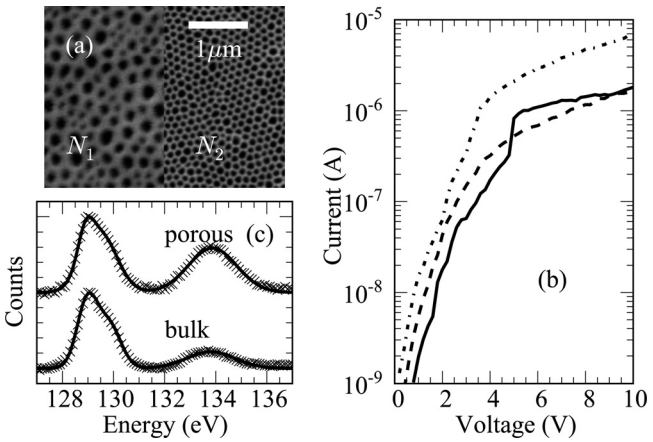

FIG. 1. (a) Electron micrograph of the surface of (100)-oriented curropores in n-type InP doped at $N_1 = 1 \times 10^{17}$ cm^{-3} (left) or $N_2 = 9 \times 10^{18}$ cm^{-3} (right). (b) Current-voltage characteristics in the dark (initial sweep, solid line; second sweep, dashed line) and under illumination at 800 nm (dashed-dotted line). (c) XPS spectra of the phosphorous 2p core-levels of (100)-oriented bulk and porous InP.

a)Electronic mail: james.lloyd-hughes@physics.ox.ac.uk.

the porous honeycomb, although a change in the contact resistance may also have an effect.

To further investigate electron transport, we measured the transmission T to far-infrared radiation using terahertz time-domain spectroscopy.[8,12] Porous membranes were mounted at normal incidence on metal disks with a 6 mm aperture and were held in vacuum (0.5 mbar) or air. Electrons and holes were injected optically using a fraction of the beam from a mode-locked Ti:sapphire laser (center wavelength 800 nm). The frequency dependence of $|T|$ before illumination is shown in Fig. 2(a) for the high-doping sample. A monotonic decrease in the absolute transmission towards higher frequencies is observed, owing to an increase in the absorption coefficient. In order to model the transmission, we adapted the effective medium theory outlined by Polder and van Santen,[13] a generalization of Maxwell-Garnet theory to ellipsoidal particle shapes. The dielectric function ϵ_h of the host medium was calculated from the Drude-Lorentz dielectric function including the lattice and plasma response, the later of which is parameterised by the free electron density n and momentum scattering time τ. The dielectric function ϵ^* of the effective medium can be determined from

$$\epsilon^* = \epsilon_h + f(\epsilon_p - \epsilon_h)\frac{2\epsilon^*}{\epsilon^* + \epsilon_p}, \quad (1)$$

where the pores are assumed to be infinitely long cylinders of relative dielectric constant $\epsilon_p = 1$ and fill fraction f. The factor $2\epsilon^*/(\epsilon^* + \epsilon_p)$ is the ratio of the radial electric field inside and outside a pore. Equation (1) yields a quadratic equation for ϵ^* that can be solved readily. Note that this expression is valid for an array of aligned pores and differs from that for cylinders oriented at random as assumed in Ref. 13. As the samples are not in the thin- or thick-film limit, the complex refractive index cannot be calculated analytically from the experimental complex electric-field transmission T. In this analysis, we input ϵ^* into an expression for the transmission that is valid for an arbitrary sample thickness. Previously, the complex conductivity of porous InP membranes was determined by numerical calculation,[9] under the assumption that the high-frequency dielectric constant was that of bulk InP (i.e., neglecting effective medium effects).

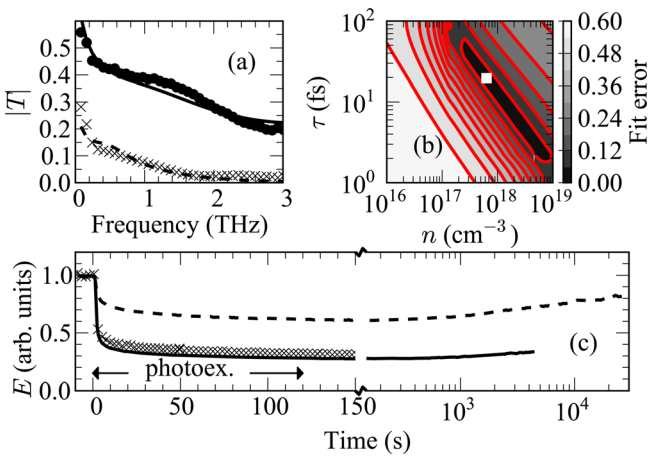

FIG. 2. THz transmission of porous InP with high doping. (a) Frequency dependence of transmission $|T|$ before (circles) and $t = 100$ s after (crosses) photoexcitation begins. Fits using the model outlined in the text ($\tau = 40$ fs) are indicated by the solid ($n = 3.0 \times 10^{17}$ cm^{-3}, $t < 0$) and dashed ($n = 9 \times 10^{18}$ cm^{-3}, $t = 100$ s) lines. (b) Root-mean-square error between model and experiment before photoexcitation at various values of τ and n. Darker regions have smaller error, and the square indicates the global minimum. (c) Peak THz electric field versus time after photoexcitation, at fluences F_1 (solid line) and F_2 (crosses) for a sample in vacuum. The dashed line is for the same sample in air at fluence F_1. The arrows indicate the photoexcitation period.

The calculated transmission [solid line in Fig. 2(a)] using $f = 0.5$, $\tau = 40$ fs, and $n = 3.0 \times 10^{17}$ cm^{-3} is in close accord with the experiment. However, an adequate fit can be obtained over a range of n and τ, as indicated by the contour plot of the root-mean-square deviation in Fig. 2(b). While the global minimum is at $\tau = 20$ fs and $n = 6.3 \times 10^{17}$ cm^{-3} (white square), the fit to experiment is good over the ranges $\tau = 40$ fs to 8 fs and $n = 3 \times 10^{17}$ cm^{-3} to 2×10^{18} cm^{-3}. A previous study using optical-pump, terahertz-probe spectroscopy found $\tau = 37$ fs for photoexcited electrons at 100 K.[10] The extracted electron density is significantly smaller than the doping level $N_d = 8 \times 10^{18}$ cm^{-3}, suggesting that the porous membrane is depleted of electrons. The transmission of the porous membranes with lower N_d was higher and showed a similar spectral shape.

Under photoexcitation at 800 nm, the THz transmission of the porous samples reduced quasi-irreversibly. In Fig. 2(c), the electric field amplitude E of the peak of the THz pulse is plotted versus measurement time t after photoexcitation, normalized to its value at $t < 0$, for a $\langle 111 \rangle$, low-doping porous material. At $t = 120$ s, the photoexcitation beam was blocked. The solid line illustrates $E(t)$ when the incident fluence F was $F_1 = 750$ nJ cm^{-2} (average power of 1.5 W, from a 4 MHz chirped-pulse Ti:sapphire laser) and the sample was held in vacuum. The initial reduction in transmission takes approximately 10 s, before reducing to 30% by $t = 100$ s.

Three possible mechanisms by which the transmission can be reduced under photoexcitation are (i) an enhanced conductivity due to photoexcited electrons and holes, (ii) a higher lattice temperature producing more intrinsic and extrinsic electrons, and (iii) a reduction in electron depletion caused by a modification of the density of surface states. The lack of a rapid recovery in E after the pump beam is blocked at $t = 120$ s rules out option (i) [photoexcited electrons] as the origin of the reduced transmission, as the electron-hole recombination time[9] in porous InP is about 5 ns. Indeed the transmission only recovers slowly, recovering to 35% by $t = 4000$ s. A thermal origin [(ii)] was discluded by photoexciting with a $\sim 10\times$ lower average power (130 mW, corresponding to a fluence of $F_2 = 14$ nJ cm^{-2}, using a 75 MHz passively mode-locked Ti:sapphire laser). The change in E with time is shown by the crosses in Fig. 2(c) and matches closely to $E(t)$ at higher fluence and average power. In air, E does not reduce as substantially (dashed line), and the recovery rate is faster.

The frequency dependent transmission at $t = 100$ s is reported by the crosses in Fig. 2(a), which can be modelled with $\tau = 40$ fs and $n = 9.0 \times 10^{18}$ cm^{-3} (dashed line). This electron density is comparable to the doping density and is about $20\times$ higher than that before photoexcitation. Note that the transmission does not reduce by the same factor because the effective medium has a high f. The $N_d = 1 \times 10^{17}$ cm^{-3} sample was fit by $n = 4.0 \times 10^{16}$ cm^{-3} before and $n = 8.0 \times 10^{16}$ cm^{-3} 100 s after photoexcitation, and exhibited

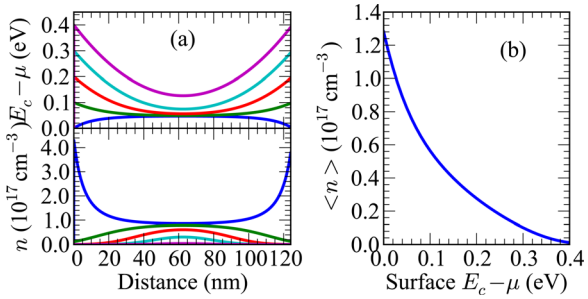

FIG. 3. (a) Conduction band energy E_c relative to the chemical potential μ, and electron density n for a 125 nm thick InP wall doped at $N_d = 1 \times 10^{17}$ cm^{-3}, for various surface pinning energies. (b) Average electron density $\langle n \rangle$ as a function of the surface pinning energy.

a similar dynamic to that in Fig. 2(c). The current flowing under dc bias is also enhanced under photoexcitation (at F_2), as shown by the current-voltage sweep taken at $t = 3$ s [dashed-dotted line in Fig. 1(b)], further supporting the increase in electron density.

In order to examine the surface composition of the porous membranes, we performed XPS using a Mg Kα X-ray source. In Fig. 1(c), the phosphorous 2p core-level spectra are shown for a reference $\langle 111 \rangle, N_d = 9 \times 10^{18}$ cm^{-3} substrate (lower crosses) and for a high porosity membrane (upper crosses) made from the same wafer. Peak energies were extracted from a fit using the sum of three Gaussians (solid lines). The lower two peaks, at 129.0 eV and 129.8 eV, correspond to the P $2p_{3/2}$ and $2p_{1/2}$ transitions[14] and are comparable for the porous and bulk samples. The feature at 133.7 eV is enhanced for the porous sample and arises from a surface oxide layer.[14] Quantatitive analysis of the relative peak intensity suggests the presence of a non-stoichiometric layer of InP_xO_y in both bulk and porous samples. The oxide In_2O_3 was discluded because of the lack of an oxygen 1s peak at 530.2 eV.[14] $\langle 100 \rangle$-oriented porous samples displayed similarly enhanced oxide spectra compared to bulk.

At semiconductor surfaces, the chemical potential is well known to be pinned by surface states. In order to quantify the influence of the surface state density σ upon the electron density n in the semiconductor, we solved the Poisson equation[15] at various surface pinning energies $E_c - \mu$, where E_c is the conduction band energy and μ is the chemical potential at the surface. Ultra-violet photoemission spectroscopy has previously determined that $E_c - \mu = 0.34 \pm 0.1$ eV for pristine $\langle 100 \rangle$ InP,[16] while for $\langle 110 \rangle$ surfaces $E_c - \mu \sim 0$ eV.[16,17] Given that the surfaces of $\langle 111 \rangle$ and $\langle 100 \rangle$ oriented pores will exhibit a variety of crystal orientations, we calculated n for $0 < E_c - \mu < 0.4$ eV. The calculated conduction band energy and electron density n are reported in Fig. 3(a) for a 125 nm thick InP wall doped at $N_d = 1 \times 10^{17}$ cm^{-3}. At $E_c - \mu = 0.4$ eV (purple lines), the conduction band is strongly bent and is raised well above the chemical potential, and the material is depleted of electrons. As $E_c - \mu$ is reduced, the bending becomes less pronounced and n increases. For $E_c - \mu < 50$ meV, electron accumulation layers form close to the surfaces. The average electron density $\langle n \rangle$ is shown in Fig. 3(b). The surface charge density σ can be linked to the electrostatic potential V via $\sigma = -\epsilon\epsilon_0 \nabla V$, where ∇V is evaluated at the semiconductor-vacuum interfaces.

The quasi-irreversible enhancement in the electron density reported in Fig. 2 can now be understood in the context of Fig. 3. A reduction in the surface pinning energy from 0.15 eV to 0.05 eV is required to increase the electron density in the semiconductor by the amount observed for the low-doping sample. A possible mechanism for a reduction in the pinning energy by $\sim$0.1 eV is as follows. The formation of indium oxides by the chemisorption of oxygen to (110) n-type InP has been reported to be enhanced under illumination with above-bandgap light,[17] possibly by electron transfer from the semiconductor into O_2^- precursor ions, which have a lower binding energy than O_2 molecules.[18] For (100) InP, the thermal desorption of In_2O_3 at 453 °C was found to shift the pinning energy from 0.1 eV (with In_2O_3 and P oxides) to 0.3 eV (just with P oxides).[19] If photoexcitation or electrical injection preferentially created In_2O_3 oxide, then the surface pinning energy would therefore be reduced. The recovery towards the original (more transmissive) state would then occur if this state was metastable in the dark.

In conclusion, the surface charge density of porous InP was found to be altered by photoexcitation. The photoinduced modification of porous semiconductors may be useful in material processing as it is a clean, dry, and area-selective method of altering the conductivity quasi-permanently. However, further work is necessary to establish the microscopic origin of the effect and its universality.

The author (J.L.) would like to thank the EPSRC (UK) for a Fellowship and P. Nandanwar for additional measurements. Partial financial support came from the SNF (Switzerland) under SCOPES Grant No. IZ73Z0_1-2804.

[1]H. Föll, S. Langa, J. Carstensen, M. Christophersen, and I. M. Tiginyanu, Adv. Mater. **15**, 183 (2003).
[2]V. V. Ursaki, N. N. Syrbu, S. Albu, V. V. Zalamai, I. M. Tiginyanu, and R. W. Boyd, Semicond. Sci. Technol. **20**, 745 (2005).
[3]I. M. Tiginyanu, I. V. Kravetsky, S. Langa, G. Marowsky, J. Monecke, and H. Föll, Phys. Status Solidi A **197**, 549 (2003).
[4]M. Reid, I. Cravetchi, R. Fedosejevs, I. M. Tiginyanu, L. Sirbu, and R. W. Boyd, Phys. Rev. B **71**, 081306(R) (2005).
[5]K. Radhanpura, S. Hargreaves, R. A. Lewis, L. Sirbu, and I. M. Tiginyanu, Appl. Phys. Lett. **97**, 181921 (2010).
[6]H. Föll, J. Carstensen, and S. Frey, J. Nanomater. **2006**, 91635 (2006).
[7]T. Sato, A. Mizohata, and T. Hashizume, J. Electrochem. Soc. **157**, H165 (2009).
[8]R. Ulbricht, E. Hendry, J. Shan, T. F. Heinz, and M. Bonn, Rev. Mod. Phys. **83**, 543 (2011).
[9]S. K. E. Merchant, J. Lloyd-Hughes, L. Sirbu, I. M. Tiginyanu, P. Parkinson, L. M. Herz, and M. B. Johnston, Nanotechnology **19**, 395704 (2008).
[10]J. Lloyd-Hughes, S. K. E. Merchant, L. Sirbu, I. M. Tiginyanu, and M. B. Johnston, Phys. Rev. B **78**, 085320 (2008).
[11]S. Langa, I. M. Tiginyanu, J. Carstensen, M. Christophersen, and H. Föll, Appl. Phys. Lett. **82**, 278 (2003).
[12]P. U. Jepsen, D. G. Cooke, and M. Koch, Laser Photonics Rev. **5**, 124 (2011).
[13]D. Polder and J. H. van Santen, Physica **12**, 257 (1946).
[14]G. Hollinger, E. Bergignat, J. Joseph, and Y. Robach, J. Vac. Sci. Technol. A **3**, 2082 (1985).
[15]S. Birner, T. Zibold, T. Andlauer, T. Kubis, M. Sabathil, A. Trellakis, and P. Vogl, IEEE Trans. Electron Devices **54**, 2137 (2007).
[16]J. M. Moison and M. Bensoussan, Surf. Sci. **168**, 68 (1986).
[17]L. Koenders, F. Bartels, H. Ullrich, and W. Monch, J. Vac. Sci. Technol. B **3**, 1107 (1985).
[18]W. Mönch, *Semiconductor Surfaces and Interfaces*, 3rd ed. (Springer, 2001).
[19]W. M. Lau, R. N. S. Sodhi, and S. Ingrey, Appl. Phys. Lett. **52**, 386 (1988).